Vertical profiles of sub-3 nm particles over the boreal forest

Katri Leino[1*], Janne Lampilahti[1], Pyry Poutanen[1], Riikka Väänänen[1], Antti Manninen[1], Stephany Buenrostro Mazon[1], Lubna Dada[1], Anna Nikandrova[1], Daniela Wimmer[1], Pasi P. Aalto[1], Lauri R. Ahonen[1], Joonas Enroth[1], Juha Kangasluoma[1], Petri Keronen[1], Frans Korhonen[1], Heikki Laakso[1], Teemu Matilainen[1], Erkki Siivola[1], Hanna E. Manninen[1,2], Katrianne Lehtipalo[1,3], Veli-Matti Kerminen[1], Tuukka Petäjä[1] and Markku Kulmala[1]

[1] Institute for Atmospheric and Earth System Research / Physics, Faculty of Science, P.O. Box 64, FI-00014 University of Helsinki, Finland

(* corresponding author's email: katri.e.leino@helsinki.fi)

[2]CERN, CH-1211Geneva 23, Switzerland.

[3]Finnish Meteorological Institute, Erik Palménin aukio 1, 00560 Helsinki, Finland

Abstract. This work presents airborne observations of sub-3 nm particles in the lower troposphere and investigates new particle formation (NPF) within an evolving boundary layer (BL). We studied particle concentrations together with supporting gas and meteorological data inside the planetary BL over a boreal forest site in Hyytiälä, Southern Finland. The analysed data were collected during three flight measurement campaigns: May-June 2015, August 2015 and April-May 2017, including 27 morning and 26 afternoon vertical profiles. As a platform for the instrumentation, we used a Cessna 172 aircraft. The analysed flight data were collected horizontally within a 30-km distance from the SMEAR II station in Hyytiälä and vertically from 100 m above ground level up to 2700 m. The number concentration of 1.5–3 nm particles was observed to be, on average, the highest near the forest canopy top and to decrease with an increasing altitude during the mornings of NPF event days. This indicates that the precursor vapours emitted by the forest play a key role in NPF in Hyytiälä. During daytime, newly-formed particles were observed to grow in size and the particle population became more homogenous within the well-mixed BL in the afternoon. During undefined days in respect to NPF, we also detected an increase in concentration of 1.5–3 nm particles in the morning but not their growth in size, which indicates an interrupted NPF process during these undefined days. Vertical mixing was typically stronger during the NPF event days than during the undefined or non-event days. The results shed light on the connection between boundary layer dynamics and NPF.

1 Introduction

One of the most important sources of secondary aerosol particles in the atmosphere is new particle formation (NPF). NPF and subsequent growth is a globally observed phenomenon (Kulmala et al., 2004; Kulmala and Kerminen, 2008; Kerminen et al., 2018). It is still partly unclear where, when and how NPF occurs in the atmosphere. Aerosol measurements on board of an aircraft can give information about the vertical, horizontal and spatial extent of the NPF in the lower atmosphere.

The planetary boundary layer (PBL) is a complex layer in the lowest part of the atmosphere, defined as the part of the troposphere that is directly connected to the Earth's surface through the exchange of momentum, heat and mass, and responds to surface forcing with a timescale of an hour or less (Stull, 2012). The PBL has a characteristic diurnal cycle, but the detailed development varies from day to day. Several meteorological, physical and chemical processes influence the spatial and temporal conditions inside the BL and thus the mixing strength and evolution of boundary layer. This gives rise to the complexity to define the exact BLH or to characterize the typical BL structure or height at a given location.

Several airborne measurements have been conducted to investigate particle number concentrations and size distributions as well as NPF inside the PBL. Over Europe, Crumeyrolle et al. (2010) observed that the horizontal extent of NPF was about 100 km or larger during the EUCAARI campaign in 2008 (Kerminen et al., 2010), while Wehner et al. (2007) estimated a corresponding scale of up to 400 km with clear horizontal variability in NPF characteristics during the SATURN campaign in 2002. The number concentrations and size distributions of naturally charged particles (air ions) were under investigation during EUCAARI-LONGREX campaign in May 2008 (Mirme et al., 2010). They reported that NPF takes place throughout the whole BL, and that the particles have formed more likely via neutral than ion-induced pathways inside the PBL.

One of the sinks of newly formed aerosol particles in the PBL is dry deposition, which is important especially for the smallest particles (Rannik et al., 2000; Lauros et al., 2011). Recently, Zha et al. (2018) studied the vertical profile of highly oxygenated organic compounds (HOMs), which are known precursors for aerosol formation (Ehn et al., 2014). They found that while the concentrations were similar below and above canopy (35 m) during well-mixed conditions, the concentrations were often clearly lower near the ground level during night-time, when temperature inversion occurred, probably due to changes in their sources and sinks (e.g. surface deposition) during stable conditions.

In addition to NPF near to the surface inside the PBL and NPF in the free troposphere (FT) (Bianchi et al., 2016), NPF has also been observed near clouds (Wehner et al., 2015). Siebert et al. (2004), Platis et al. (2016) and Chen et al. (2018) observed NPF to initiate on top of the boundary layer in a capping inversion followed by subsequent mixing of the freshly formed particles throughout the well-mixed boundary layer. Wehner et al. (2010) studied NPF in the residual layer and observed that turbulent mixing is likely to lead to a local super saturation of possible precursor gases, which is essential for NPF. The particles were formed in parts of the residual layer and subsequently entrained into the BL where they were detected at the surface.

NPF events are frequently occurring over the boreal forest region in Southern Finland (Kulmala et al., 2001; Dal Maso et al., 2005; Kulmala et al., 2013). In addition to ground-based measurements at the SMEAR II station (61°51'N, 24°17'E, 181 m above sea level, Hari and Kulmala, 2005), which have been conducted continuously since 1996, also airborne measurements of aerosol particles have been carried out near the station since the year 2003 during several campaigns using a small aircraft (O'Dowd et al., 2009; Schobesberger et al., 2013) and a hot-air balloon (Laakso et al., 2007). Laakso et al. (2007) observed NPF to occur in the mixed BL, but also in the FT with no connection to the BL nucleation. O'Dowd et al. (2009) observed NPF throughout the BL over the SMEAR II, with the nucleation mode number concentration peaking first above the forest canopy. Schobesberger et al. (2013) observed NPF inside the PBL. High concentrations of nucleation mode particles were also found in the upper parts of the PBL, which indicates that nucleation does not necessarily occur only close to the surface. The vertical profiles of small particles in mixing BL at SMEAR II were also modelled by Boy et al. (2006). Their results predicted that the maximum of newly formed clusters and particle concentrations is located near the ground level.

In this study, we investigate the vertical variation of 1.5–3 nm and 3–10 nm particles from the ground level up to 3 kilometres during different kind of days in relation to the occurrence of NPF at the ground level, as well as the vertical mixing of a particle population within the evolving BL. The dataset was collected during three measurement flight campaigns, in spring 2015, August 2015 and in spring 2017, within a 30-km distance from the SMEAR II station. The results are compared to the data measured on the ground level at the station. Traditional NPF event classification is used to classify studied days as NPF events, non-events and undefined days (Dal Maso et al., 2005).

The questions we would like to answer are: Which kind of characteristics do we have in the vertical profile of small particles?; How do these profiles differ between the NPF event, non-event and undefined days?; Where do new particles form and how does the strength of turbulent mixing affect

particle concentrations?; What is the median concentration of small particles inside the BL during the NPF event, non-event and undefined days, and how well do the results agree with the values measured on the ground level?

2 Materials and methods

2.1 Measurements on board Cessna

As a platform for aerosol instruments, we used a light one-engine Cessna FR172F aircraft. The measurement instruments were installed on an aluminium rack at the middle part inside the plane's cabin (Fig. 1). A steel inlet line (with 32 mm inner diameter) was mounted onto the top of the rack and lifted in and out from the window in the left side of the plane. The sample was collected from a 50-cm distance from the fuselage of the plane. The main flow in the steel tube was kept constant at 47 l min^{-1} during the measurement flight and was produced by suction in the venturi and forward motion of the airplane. Each instrument took their actual inlet flow from the central line of the main flow, minimizing the diffusional losses of the smallest particles. The measurements were performed with an airspeed of 125 km/h. More details about partly the same instrumentation and layout can be found in Schobesberger et al. (2013) and Väänänen et al. (2016). The data were collected within a 30-km distance from SMEAR II station and the area is covered mainly by coniferous forest.

2.1.1 Instrumentation

The main instrumentation for this study consisted of several different particle counters. An ultrafine condensation particle counter (uCPC, model TSI-3776) is an instrument that detects the total concentration of particles larger than about 3 nm in diameter. Particles larger than the threshold diameter are grown into large droplets by condensing butanol vapour onto their surface, after which they are detected optically with a laser-diode photodetector. The ultrafine CPC has an internal vacuum pump that draws the aerosol sample with flow rate of 1.5 l min^{-1} into the instrument.

Airmodus Ltd has developed a mixing-type Particle Size Magnifier (PSM). The instrument is able to detect directly sub-3 nm atmospheric particles using diethylene glycol (DEG) as condensing fluid (Vanhanen et al., 2011). Compared with typically-used working fluids in CPCs, water and butanol, the advantages of using DEG as condensing fluid are its lower saturation vapour pressure and higher surface tension, which enables to detect particles down to 1 nm. The PSM requires a separate water or butanol counter (CPC) for detecting optically the grown particles. The PSM in this study was a model A10, operating with a butanol CPC (model TSI-3010). During the flight measurements

presented here, the instrument was used in fixed saturator flow rate mode measuring the total particle concentration with a 1.5 nm cut-off size.

The instrumentation included also a custom-built Scanning Mobility Particle Sizer (SMPS), which measures the particle number size distribution in the diameter size range of 10–400 nm with a 2-min time resolution. Before the classification of an aerosol population, the particles are transported to a radioactive source where they reach a constant bipolar charge equilibrium. The SMPS contains a differential mobility analyser (DMA, Hauke type), while particle number concentrations are measured with a butanol CPC (model TSI-3010).

The concentrations of water vapour (H_2O) and carbon dioxide (CO_2) were measured with a Li-Cor (LI-840) gas analyser located in the instrumentation rack. Basic meteorological variables, including the ambient temperature (with PT-100 temperature sensor), relative humidity (RH) (with Rotronic HygroClip-S sensor) and static pressure (with Vaisala PTB100B), were measured. Pressure was measured inside the plane while the temperature and RH sensor was located in the right wing of the plane. The location of plane was recorded by a GPS receiver.

2.2 SMEAR II research station

A research Station for Measuring Ecosystem-Atmospheric Relations (SMEAR) II in Hyytiälä, Southern Finland, was established in 1995 (see Hari and Kulmala, 2005). The station is equipped with several aerosol and gas instruments together with flux, irradiation and meteorological measurements. The long-term measurements give reliable and comprehensive knowledge about ambient conditions at a relatively clean coniferous forest site. The station includes ground-based measurements, tower measurements at the 35-m height above the ground level right above the canopy, and measurements conducted from a mast at different altitudes up to 128 m.

In this study, we mainly used particle data from the ground level as a reference data to which we compare our flight measurement data. The number concentrations in the size range of 1.5–3 nm were calculated from the difference between the measured total particle concentration at the 1.5 nm cut-off size (from the PSM) and total concentration at the 3 nm cut-off size (from DMPS). The distance between the PSM and DMPS is vertically a few meters and horizontally a few tens of meters, which causes some uncertainties in 1.5–3 nm particle number concentrations, especially during poorly-mixed BL times in the morning when the two instruments do not always measure the same air mass.

The sensible heat flux (SHF) was measured at the at 23-m height, and we used these data to get qualitative information on the strength of vertical mixing in the measured air masses.

5

2.3 Data analysis

The particle number concentration in the size range of 1.5–3 nm was calculated as the difference of the total particle concentrations measured with the PSM and uCPC on board the Cessna. The cut-off sizes of these instruments were 1.5 nm and 3 nm. The cut-off size of the SMPS was 10 nm. The number concentration in the size range of 3–10 nm was calculated as the difference in the total particle number concentrations measured with uCPC and SMPS.

Total particle number concentrations measured on board the Cessna were first converted into standard temperature and pressure conditions (STP, 273.15K, 100 kPa) and then were corrected with the maximum detection efficiency of the instrument based on laboratory calibrations. The maximum detection efficiency of the PSM used in airborne measurement was 0.75 and that of uCPC was 0.99. The maximum detection efficiencies of the PSMs used at the station were 0.8. Finally, the particle number concentrations were corrected with respect to diffusional losses in the inlet part (Fig. 1) and inside the sampling lines on the plane, assuming a constant correction factor for each size bin. The ground and tower data were assumed to have negligible inlet line losses because of core sampling (Kangasluoma et al., 2016). The correction factor for the inlet part was 0.716 for 1.5–3 nm particles and 0.720 for 3–10 nm particles based on simulation results using COMSOL Multiphysics software. Penetration efficiencies through the sampling lines were 0.70 and 0.88 in the size ranges of 1.5–3 nm and 3–10 nm, respectively.

All the results presented here are reported vertically as meters above the ground level, and all the data were collected from within a distance of 30 km from the SMEAR II station in Hyytiälä. A typical measurement flight includes a linear ascent from 100–200 m (a.g.l.) up to the FT region, 2500–3500 m, and a descent back near to the canopy top level.

In this study, we analysed altogether 53 measurement profiles during 18 days. The flights were conducted during three measurement campaigns: May-June 2015, August 2015 and April-May 2017, either in the morning (7:00–12:00, UTC+2) or in the afternoon (12:00–15:00) time. The days were classified as event, non-event or undefined days based on the NPF event classification method by Dal Maso et al. (2005).

Well-mixed boundary layers are capped by a stable layer. The boundary layer height (BLH) was visually estimated from the in-situ measurements onboard the Cessna aircraft for each vertical measurement profile. The BLH was estimated from minimum vertical gradient in H_2O and RH, and maximum vertical gradient in the potential temperature. The estimated BLH was evaluated visually with Doppler lidar profiles when possible (due to very low lidar signal-to-noise ratio in the clean-air

6

environment), and was found to agree very well. When the sun is rising, the mixing of air mass starts from near the ground, and aerosol particles originating from surface get mixed upwards within the rising mixed layer. Inside the mixing layer, higher concentrations of H_2O are sometimes seen when the turbulence mixes up the moisture from the surface. CO_2 tends to be higher in the morning boundary layer due to respiration and decreases in the residual layer. The vertical profile of the potential temperature is almost constant in the surface mixed layer and rapidly increases with an increasing altitude under stable conditions.

2.4 Uncertainties

As described above, all the results were converted into standard temperature and pressure (STP, 100 kPa, 273.15K) conditions and corrected for the instrumental maximum detection efficiency and line losses according to the laboratory characterizations of the flight setup. However, there are several factors causing uncertainties in the measured concentrations. The flight speed, main flow rate, air pressure, relative humidity and temperature are changing rapidly during a flight, which can cause variations in the inlet flows and the performance of the instruments. It is poorly known how the uCPC and PSM behave under quickly varying operational conditions. The reduced pressure at high altitudes may change the maximum detection efficiency and cut-off size of laminar flow CPCs (e.g. Zhang and Liu, 1991; Herrman and Wiedensohler, 2001). The pressure effect on the PSM cut-off size has been observed to be small (< 0.1 nm until 60 kPa) compared to the uncertainty caused by a changing relative humidity and particle composition (Kangasluoma et al., 2016). We measured up to altitudes with the pressure going down to ~70 kPa, which gives an uncertainty of ±5 % for the aerosol flow rate of the CPC 3776, and thus directly to the concentrations, as shown by Takegawa et al. (2017), Fig 3. In addition, we compared the concentrations measured by PSM, uCPC and SMPS in the FT where the occurrence of small particles (below 10 nm, that has been under discussion in this paper) is very low. These concentrations matched well with each other, so we may assume that the pressure effect to the measured concentrations for any of the instruments was not significant in our study.

Because of the uncertainties in the instrument cut-off sizes, the true size range of the 1.5–3 nm concentration may vary with altitude and between different flights. This would also slightly affect the particle sampling losses, which were here assumed to be constant for the whole size range, although in reality there is a size dependency. Because of these uncertainties in the determined concentrations, we should focus on the relative behaviour of median values rather than absolute concentrations.

3   Results and discussion

The flight days were divided into event, non-event and undefined days based on the NPF event classification by Dal Maso et al. (2005). Based on this classification on the ground level, the vertical profiles of particles in the size ranges of 1.5–3 nm and 3–10 nm were studied separately in each type of days. During event and undefined days, we also looked at differences between the morning and afternoon times. The number of flights during non-event days is low (two vertical profiles), because cloudiness makes the operation of the aircraft impossible. Non-event days are mostly cloudy in Hyytiälä (Dada et al., 2017).

For the flight days, when we have comparable particle data from the ground station, we calculated the median values of 1.5–3 nm particle concentration both inside BL on board the Cessna and on the ground level. The boundary layer height was estimated for every vertical measurement profile.

3.1   General features and vertical profiles

The median values of particle concentrations, sensible heat flux (SHF), median of measurement height and estimated BLH was calculated for the 27 cases when comparable data were available at the SMEAR II station (Table 1). The values onboard aircraft (inside the BL) indicates here the observations on board Cessna, which means that the minimum limit for altitude was around 100 m from ground level. The values on the ground level were measured inside the forest canopy.

On average, we found that the concentration of 1.5–3 nm particles were higher onboard aircraft (inside the BL) (1400 cm^{-3}) than on the ground station level (1100 cm^{-3}) (hereafter referred to as 'ground'). The observation of having somewhat lower concentrations of small particles at ground level is probably due to higher sinks of particles and their precursors inside the canopy compared with above-canopy air (Tammet et al., 2006; Zha et al., 2018). The values were the highest on NPF event days (1500 cm^{-3} onboard aircraft (inside the BL) and 1300 cm^{-3} on the ground) and undefined days (1450 cm^{-3} onboard aircraft (inside the BL) and 1130 cm^{-3} on the ground) and clearly the lowest on non-event day both onboard aircraft (inside the BL) (890 cm^{-3}) and on the ground level (740 cm^{-3}). It should be noted that both of two non-event profiles were measured during the same afternoon in the spring of 2015.

The median BLH of all the profiles was 1400 m, being lower in the morning (1100 m) and higher during the afternoon flights (2000 m). Indicative of stronger vertical mixing, the median value of the

250 sensible heat flux (SHF) was the highest on the NPF event days, especially during the afternoon (286
251 W m^{-2}).

252 Figure 2 shows the median vertical profiles of the total particle number concentration in the size
253 ranges of 1.5–3 nm and 3–10 nm separately for the NPF event days, undefined days and one non-
254 event day. The profiles typically contain data from 100 m up to 2700 m above the ground level. It is
255 noticeable that the non-event profile consists of only two vertical profiles and that both of them were
256 measured in the same afternoon. We found that airborne 1.5–3 nm particle concentrations were
257 similar between the event and undefined days, whereas substantially lower concentrations were
258 observed on non-event day. We also observed that during the event days there were clearly more 3–
259 10 nm particles inside the BL (onboard aircraft) than during undefined days (Fig. 2a and 2b). The
260 reason for this could be that during the undefined days the formation of sub-3 nm particles took place,
261 yet the conditions were not suitable for the particle growth to larger sizes (see Buenrostro Mazon et
262 al., 2009; Kulmala et al., 2013). Our findings are consistent with earlier observations of high sub-3
263 nm particle concentrations in Hyytiälä on both event and undefined days compared with non-event
264 days (Lehtipalo et al., 2009; Dada et al., 2017).

265 During the NPF event days, median, 25th and 75th percentiles show that the concentration of sub-3
266 nm particles was relatively the highest right above the canopy top. This indicates that the sources of
267 particles and their precursor vapors are near the ground level. During the undefined days, the origin
268 of sub-3 nm particles was not necessarily at the ground level, as their concentration decreased right
269 above the ground level (from 100 m to 200 m). In addition, reviewing the median values in Table 1,
270 the concentration of 1.5–3 nm particles was observed to be higher inside the BL (onboard aircraft)
271 during morning times of undefined days (2800 cm^{-3}) than during afternoon times (1150 cm^{-3}),
272 oppositely to event days (1070 cm^{-3} and 3020 cm^{-3}, respectively), which supports this hypothesis
273 (Table 1). The concentrations of both sub-3 nm and 3–10 nm particles were very low during the non-
274 event days and we did not observe any clear layers for these particles. However, it should be noted
275 that our study included only two such profiles, since the flight measurements were not possible to
276 conduct during non-event days due to meteorological conditions, especially cloudiness.

277 The measurement flights were conducted either in the morning (7:00–12:00, UTC+2) or in the
278 afternoon (12:00–15:00). We studied the median vertical particle concentrations separately for those
279 two times in order to estimate the effect of mixing strength on the vertical profile of particles on NPF
280 event and undefined days. As expected based on observed SHF fluxes, we found that the
281 concentrations of 1.5–3 nm particles inside the BL (onboard aircraft) were, on average, most
282 homogenous vertically during the afternoons of the NPF event days (Fig. 3).

9

On NPF event days, we can see an interesting layer of 3–10 nm particles in the morning above the BL at 2400 m. From this layer, the particles can mix down into the evolving BL. A similar behavior is seen on undefined days, when the increase in concentration of 1.5–3 nm particles is observed in layer right below 2500 m in the morning and the particles are grown in size and mix downward until afternoon.

3.2 Diurnal variation of particle concentration at different altitudes in the lower atmosphere

We studied the median diurnal variation of total particle concentration (all particles > 1.5 nm) and separately particle concentration in size range of 1.5–3 nm at different altitudes from around 100 m to 2700 m above the ground level around the SMEAR II station area. The study included 17 vertical measurement profiles during event days and 34 during undefined days. From Fig. 4a it can be seen that the total particle number concentration over all measurement profiles was the highest near the ground in the morning. The aerosol population mixed with cleaner air within the evolving BL after the morning, which led to a decreasing particle number concentration, whereas the concentration increased again towards the afternoon, presumably as a result of NPF. The highest particle number concentrations were observed at 11:30–14:30 inside the BL (onboard aircraft), which coincides with the peak time of NPF in Hyytiälä (Dada et al., 2018).

The sub-3 nm particle number concentrations (Fig. 4b) were the highest in the morning near the ground level, with a second maximum around the noon. Later in the afternoon, the sub-3 nm particle concentration was clearly lower, probably because these particles apparently grew efficiently to larger sizes and contributed significantly to the total particle concentration (Yli-Juuti et al., 2011). Both total particles and sub-3 nm particles had the highest concentrations near the ground level throughout the day, even though especially the total particle population seems to have been spread within the whole mixed layer.

Figure 4c shows the data availability for this analysis. It is noticeable that the number of data in each 100 m-half-an-hour cell varies considerably. In addition, one intense NPF event day with strong particle formation in the early morning dominated the distribution due to the low number of flights at around 7:00–8:00. Most of the data were collected either during the morning (8:30–11:30) or afternoon (13:30–15:00). As we know, also the BLH, mixing of air and meteorological conditions can differ significantly even within one day, and especially so between the NPF event and undefined days.

10

3.3 Case study – NPF in evolving BL

The 13th of August 2015 was an intense NPF event day in Hyytiälä (Fig. 5a). During that day we conducted two measurement flights around the SMEAR II station and observed the particle concentration in size range of 1.5–3 nm to follow the development of BL and turbulent mixing (Fig. 6a, 6c, 7a, 7c). During the first measurement flight at 7:30–9:00, we observed a clear layer of 3–10 nm particles near the FT region above 2300 m. These particles were mixed down before the afternoon flight, as this population was not anymore observed during that flight. The negative (downwards) particle flux at SMEAR II after 12:00 supports this hypothesis (Fig. 5b).

The estimated BLH was ~500–700 meters during the first flight in the morning and had risen up to 1500–1700 meters until afternoon flight. Below the FT, the vertical variation of the 1.5–3 nm particle concentration was larger compared to the stable conditions in FT. The median of concentration of 1.5–3 nm particles inside the BL (onboard aircraft) decreased from the morning flight (7300 cm^{-3} during the ascent and 6300 cm^{-3} during the descent, Fig. 6a and 6c) to the afternoon flight (~2500 cm^{-3}, Fig. 7a and 7c), whereas 3–10 nm particles seemed to behave in an opposite manner (350 cm^{-3}, 200 cm^{-3}, 850 cm^{-3} and 1450 cm^{-3}). The sub-3 nm particle concentrations were clearly higher inside the BL (onboard aircraft) than in the FT, and the concentration increased towards the ground. This is consistent with organic vapors, emitted from the ground vegetation, participating in NPF and growth (Kulmala et al., 2013; Ehn et al., 2014).

4 Conclusions

Small 1.5–3 nm particles were observed inside the convective BL on-board a Cessna aircraft. On average, the highest concentrations of sub-3 nm particles were found during NPF event mornings above the forest canopy top. This points towards the forest being an important source of the precursor vapors for newly formed particles. Due to the convective mixing inside BL, small particles near the ground started to mix up while sub-10 nm particles mixed down from the FT region. Strong vertical mixing was more typical for the NPF event days than for the undefined and non-event days, especially during the afternoon. The concentration of sub-3 nm particles was clearly higher inside the BL (onboard aircraft) on both NPF event days and undefined days compared with one non-event day, but their vertical variation was somewhat different, reflecting the different mixing conditions. The event days also showed a clear increase of 3–10 nm particles in the afternoon, which was missing on undefined days when the NPF process had been interrupted.

We found that airborne and on-ground median concentrations of sub-3 nm particles were mostly in good agreement. Some differences still existed, which can be explained by poor vertical mixing of air, changes in air mass origins and regional variations. The concentrations of sub-3 nm particles on the ground were, on average, somewhat lower than airborne observations, which indicates a higher sink for these particles inside the forest canopy.

This study increases our understanding of the first steps of atmospheric NPF inside the whole BL and the connections between atmospheric mixing and NPF. The next step would be to investigate different formation pathways in more detail. To achieve this, it would be important to find out also the chemical composition of particles above the ground level so that we could assess more specifically the possible sources of the precursor gases. In addition, the contribution of mesoscale convection-induced movement, like roll vortices, to NPF is currently under investigation.

References

Boy, M., Hellmuth, O., Korhonen, H., Nilsson, E.D., Revelle, D., Turnipseed, A., Arnold, F. and Kulmala, M.: MALTE – model to predict new aerosol formation in the lower troposphere, Atmos. Chem. Phys., 6, 4499–4517, 2006.

Bianchi, F., Trostl, J., Junninen, H., Frege, C., Henne, S., Hoyle, C. R., Molteni, U., Herrmann, E., Adamov, A., Bukowiecki, N., Chen, X., Duplissy, J., Gysel, M., Hutterli, M., Kangasluoma, J., Kontkanen, J., Kuerten, A., Manninen, H. E., Muench, S., Perakyla, O., Petaja, T., Rondo, L., Williamson, C., Weingartner, E., Curtius, J., Worsnop, D. R., Kulmala, M., Dommen, J., and

376   Baltensperger, U.: New particle formation in the free troposphere: A question of chemistry and
377   timing, Science, 352, 1109–1112, 2016.

378   Buenrostro Mazon, S., Riipinen, I., Schultz, D.M., Valtanen, M., Dal Maso, M., Sogacheva, L.,
379   Junninen, H., Nieminen, T., Kerminen, V.-M. and Kulmala, M.: Classifying previously
380   undefined days from eleven years of aerosol-particle-size distribution data from the SMEAR II
381   station, Hyytiälä, Finland, Atmos. Chem. Phys., 9, 667–676, 2009.

382   Chen, H., Hodshire, A.L., Ortega, J., Greenberg, J., McMurry, P.H., Carlton, A.G., Pierce, J.R.,
383   Hanson, D.R. and Smith, J.N.: Vertically resolved concentration and liquid water content of
384   atmospheric nanoparticles at the US DOE Southern Great Plains site, Atmos. Chem. Phys.,
385   18, 311–326, 2018.

386   Crumeyrolle, S., Manninen, H., Sellegri, K., Roberts, G., Gomes, L., Kulmala, M., Weigel, R., Laj,
387   P. and Schwarzenboeck, A.: New particle formation events measured on board the ATR-42
388   aircraft during the EUCAARI campaign, Atmos. Chem. Phys., 10, 14, 2010.

389   Dada, L., Paasonen, P., Nieminen, T., Buenrostro Mazon, S., Kontkanen, J., Peräkylä, P., Lehtipalo,
390   K., Hussein, T., Petäjä T., Kerminen, V.-M., Bäck, J. and Kulmala, M.: Long-term analysis of
391   clear-sky new particle formation events and nonevents in Hyytiälä, Atmos. Chem. Phys., 17,
392   6227–6241, 2017.

393   Dada L., Chellapermal R., Buenrostro Mazon S., Paasonen P., Lampilahti J., Manninen H. E.,
394   Junninen H., Petäjä T., Kerminen V.-M. and Kulmala M.: Refined classification and
395   characterization of atmospheric new-particle formation events using air ions, Atmos. Chem.
396   Phys. 18, 17883–17893, 2018.

397   Dal Maso, M., Kulmala, M., Riipinen, I., Wagner, R., Hussein, T., Aalto, P.P. and Lehtinen, K.E.J.:
398   Formation and growth of fresh atmospheric aerosols: eight years of aerosol size distribution
399   data from SMEAR II, Hyytiälä, Finland, Boreal Environ. Res., 10, 323–336, 2005.

400   Ehn, M., Thornton, J. A., Kleist, E., Sipilä, M., Junninen, H., Pullinen, I., Springer, M., Rubach, F.,
401   Tillmann, R., Lee, B., Lopez-Hilfiker, F., Andres, S., Acir, I.-H., Rissanen, M., Jokinen, T.,
402   Schobesberger, S., Kangasluoma, J., Kontkanen, J., Nieminen, T., Kurtén, T., Nielsen, L. B.,
403   Jørgensen, S., Kjaergaard, H. G., Canagaratna, M., Maso, M. D., Berndt, T., Petäjä, T., Wahner,
404   A., Kerminen, V.-M., Kulmala, M., Worsnop, D. R., Wildt, J. and Mentel, T. F.: A large source
405   of low-volatility secondary organic aerosol, Nature, 506(7489), 476–479, 2014.

406 Hari P. and Kulmala M.: Station for Measuring Ecosystem-Atmosphere Relations (SMEAR II),
407   Boreal Environ. Res., 10, 315–322, 2005.

408 Hermann, M. and Wiedensohler, A.: Counting efficiency of condensation particle counters at low-
409   pressures with illustrative data from the upper troposphere, J. Aerosol Sci., 32, 8, 975–991,
410   2001.

411 Kangasluoma, J., Franchin, A., Duplissy, J., Ahonen, L., Korhonen, F., Attoui, M., Mikkilä, J.,
412   Lehtipalo, K., Vanhanen, J., Kulmala, M. and Petäjä, T.: Operation of the Airmodus A11 nano
413   Condensation Nucleus Counter at various inlet pressures and various operation temperatures,
414   and design of a new inlet system, Atmos. Meas. Tech., 9, 2977–2988, 2016.

415 Kerminen, V.-M., V.-M, Petäjä, T., Manninen, H.E., Paasonen, P., Nieminen, T., Sipilä, M.,
416   Junninen, H., Ehn, M., Gagné, S., Laakso, L., Riipinen, I., Vehkamäki, H., Kurten, T., Ortega,
417   K., Dal Maso, M., Brus, D., Hyvärinen, A., Lihavainen, H., Leppä, J., Lehtinen, K.E.J., Mirme,
418   A., Mirme, S., Hõrrak, U., Berndt, T., Stratmann, F., Birmili, W., Wiedensohler, A., Metzger,
419   A., Dommen, J., Baltensperger, U., Kiendler-Scharr, A., Mentel, T.F., Wildt, J., Winkler, P.M.,
420   Wagner, P.E., Petzold, A., Minikin, A., Plass-Dülmer, C., Pöschl, U., Laaksonen, A. and
421   Kulmala, M.: Atmospheric nucleation: highlights of the EUCAARI project and future
422   directions, Atmos. Chem. Phys., 10, 10829–10848, 2010.

423 Kerminen V.-M., Chen, X., Vakkari, V., Petäjä, T., Kulmala, M. and Bianchi, F.: Atmospheric new
424   particle formation: a review of observations, Environ. Res. Lett., 13, 103003, 2018.

425 Kulmala, M., Hämeri, K., Aalto, P.P., Mäkelä, J.M., Pirjola, L., Nilsson, E.D., Buzorius, G., Rannik,
426   Ü., Dal Maso, M., Seidl, W., Hoffman, T., Janson, R., Hansson, H.-C., Viisanen, Y., Laaksonen,
427   A. and O'Dowd, C.D.: Overview of the international project on biogenic aerosol formation in
428   the boreal forest (BIOFAR), Tellus, 53, 4, 2001.

429 Kulmala, M. and Kerminen, V.-M.: On the formation and growth of atmospheric nanoparticles,
430   Atmos. Res., 90, 2–4, 132–150, 2008.

431 Kulmala, M., Kontkanen, J., Junninen, H., Lehtipalo, K., Manninen, H.E., Nieminen, T., Petäjä, T.,
432   Sipilä, M., Schobesberger, S., Rantala, P., Franchin, A., Jokinen, T., Järvinen, E., Äijälä, M.,
433   Kangasluoma J., Hakala, J., Aalto, P.P., Paasonen, P., Mikkilä, J., Vanhanen, J., Aalto, J.,
434   Hakola, H., Makkonen, U., Ruuskanen, T., Mauldin, R.L., Duplissy, J., Vehkamäki, H., Bäck,
435   J., Kortelainen, A., Riipinen, I., Kurtén, T., Johnson, M.V., Smith, J.N., Ehn, M., Mentel, T.F.,

436   Lehtinen, K.E.J., Laaksonen, A., Kerminen, V.-M. and Worsnop, D.R.: Direct observations of
437   atmospheric aerosol nucleation, Science, 339, 943–946, 2013.

438 Kulmala, M., Vehkamäki, H., Petäjä, T., Dal Maso, M., Lauri, A., Kerminen, V.-M., Birmili, W. and
439   McMurry, P.H.: Formation and growth rates of ultrafine atmospheric particles: A review of
440   observations, J. Aerosol Sci., 35, 143–176, 2004.

441 Laakso, L., Gronholm, T., Kulmala, L., Haapanala, S., Hirsikko, A., Lovejoy, E. R., Kazil, J., Kurten,
442   T., Boy, M., Nilsson, E. D., Sogachev, A., Riipinen, I., Stratmann, F. and Kulmala, M.: Hot-air
443   balloon as a platform for boundary layer profile measurements during particle formation, Boreal
444   Environ. Res., 12, 279–294, 2007.

445 Lauros, J., Sogachev, A., Smolander, S., Vuollekoski, H., Sihto, S.-L., Mammarella, I., Laakso, L.,
446   Rannik, Ü. and Boy, M.: Particle concentration and flux dynamics in the atmospheric boundary
447   layer as the indicator of formation mechanism, Atmos. Chem. Phys., 11, 5591–5601, 2011.

448 Lehtipalo, K., Sipilä, M., Riipinen, I., Nieminen, T. and Kulmala, M.: Analysis of atmospheric neutral
449   and charged molecular clusters in boreal forest using pulse-height CPC, Atmos. Chem. Phys.,
450   9, 4177–4184, 2009.

451 Mirme, S., Mirme, A., Minikin, A., Petzold, A., Hõrrak, U., Kerminen, V.-M. and Kulmala, M.:
452   Atmospheric sub-3 nm particles at high altitudes, Atmos. Chem. Phys., 10, 437–451, 2010.

453 O'Dowd, C., Yoon, Y., Junkermann, W., Aalto, P., Kulmala, M., Lihavainen, H., and Viisanen, Y.:
454   Airborne measurements of nucleation mode particles II: boreal forest nucleation events, Atmos.
455   Chem. Phys., 9, 2009.

456 Platis, A., Altstäder, B., Wehner, B., Wildmann, N., Lampert, A., Hermann, M., Birmili, W. and
457   Bange, J.: An observational case study on the influence of atmospheric boundary-layer
458   dynamics on new particle formation, Boundary-Layer Meteorol., 158, 1, 67–92, 2016.

459 Rannik, Ü., Petäjä, T., Buzorius, G., Aalto, P., Vesala, T. and Kulmala, M.: Deposition Velocities of
460   Nucleation Mode Particles into a Scots Pine Forest, Environ. Chem. Phys., 22, 97–102, 2000.

461 Schobesberger, S., Väänänen, R., Leino, K., Virkkula, A., Backman, J., Pohja, T., Siivola, E.,
462   Franchin, A., Mikkila, J., Paramonov, M., Aalto, P. P., Krejci, R., Petaja, T. and Kulmala, M.:
463   Airborne measurements over the boreal forest of southern Finland during new particle
464   formation events in 2009 and 2010, Boreal Environ. Res., 18, 145–163, 2013.

15

465 Siebert, H., Stratmann, F. and Wehner, B.: First observations of increased ultrafine particle number
466   concentrations near the inversion of a continental planetary boundary layer and its relation to
467   ground-based measurements, Geophys. Res. Lett., 31, 9, 2004.

468 Stull, R. B.: An introduction to boundary layer meteorology, Springer Science & Business Media,
469   2012.

470 Takegawa, N., Iida, K. and Sakurai, H.: Modification and laboratory evaluation of a TSI ultrafine
471   condensation particle counter (Model 3776) for airborne measurements, Aerosol Sci. Tech., 51,
472   2, 235–245, 2017.

473 Tammet, H., Hõrrak, U., Laakso, L. and Kulmala, M.: Factors of air ion balance in a coniferous forest
474   according to measurements in Hyytiälä, Finland, Atmos. Chem. Phys., 6, 3377–3390, 2006.

475 Vanhanen, J., Mikkilä, J., Lehtipalo, K., Sipilä, M., Manninen, H., Siivola, E., Petäjä, T., and
476   Kulmala, M.: Particle size magnifier for nano-CN detection, Aerosol Sci. Tech., 45, 2011.

477 Väänänen, R., Krejci, R., Manninen, H.E., Manninen, A., Lampilahti, J., Buenrostro Mazon, S.,
478   Nieminen, T., Yli-Juuti, T., Kontkanen, J., Asmi, A., Aalto, P.P., Keronen, P., Pohja, T.,
479   O'Connor, E., Kerminen, V.-M., Petäjä, T. and Kulmala, M.: Vertical and horizontal variation
480   of aerosol number size distribution in the boreal environment, Atmos. Chem. Phys. Discuss.,
481   doi:10.5194/acp-2016-556, 2016.

482 Wehner, B., Siebert, H., Stratmann, F., Tuch, T., Wiedensohler, A., Petäjä, T., Dal Maso, M. and
483   Kulmala, M.: Horizontal homogeneity and vertical extent of new particle formation events,
484   Tellus, 59, 3, 362–371, 2007.

485 Wehner, B., Wehner, F., Ditas, F., Shaw, R.A., Kulmala, M. and Siebert, H.: Observations of new
486   particles formation in enhanced UV irradiance zones near cumulus clouds, Atmos. Chem.
487   Phys., 15, 11701–11711, 2015.

488 Wehner, B., Siebert, H., Ansmann, A., Ditas, F., Seifert, P., Stratmann, F., Wiedensohler, A.,
489   Apituley, A., Shaw, R., and Manninen, H. E.: Observations of turbulence-induced new particle
490   formation in the residual layer, Atmos. Chem. Phys., 10, 4319–4330, 2010.

491 Yli-Juuti, T., Nieminen, T., Hirsikko, A., Aalto, P.P., Asmi, E., Hõrrak, U., Manninen, H.E.,
492   Patokoski, J., Dal Maso, M., Petäjä, T., Rinne, J., Kulmala, M. and Riipinen, I.: Growth rates
493   of nucleation mode particles in Hyytiälä during 2003–2009: variation with particles size,

494   season, data analysis method and ambient conditions, Atmos. Chem. Phys., 11, 12865–12886,
495   2011.

496 Zha, Q., Yan, C., Junninen, H., Riva, M., Sarnela, N., Aalto, J., Quéléver, L., Schallhart, S., Dada,
497   L., Heikkinen, L., Peräkylä, O., Zou, J., Rose, C., Wang, Y., Mammarella, I., Katul, G., Vesala,
498   T., Worsnop, D.R., Kulmala, M., Petäjä, T., Bianchi, F. and Ehn, M.: Vertical characterization
499   of highly oxygenated molecules (HOMs) below and above a boreal forest canopy, Atmos.
500   Chem. Phys., 18, 17437–17450, 2018.

501 Zhang, Z. Q. and Liu, B. Y. H.: Performance of Tsi 3760 Condensation Nuclei Counter at Reduced
502   Pressures and Flow-Rates, Aerosol Sci. Tech., 15, 228–238, 1991.

503 **Tables**

504

505 Table 1. Numerical statistics about boundary layer height (BLH) and sensible heat flux (SHF)

506 indicating the mixing of air mass, and concentrations of 1.5–3 nm particles during measurement

507 flights in 2015 and 2017. The morning flights have been conducted between 7:00–12:00 o'clock and

508 afternoon flights at 12:00–15:00 o'clock. The low number of flights during non-event days is caused

509 by the cloudiness which makes the operation of the aircraft impossible.

	Number of flight profiles	Median conc. (1.5–3 nm) inside BL onboard Cessna [cm^{-3}]	Median conc. (1.5–3 nm) on ground level [cm^{-3}]	Median BLH [m]	Median SHF [W m^{-2}]	Median height [m a.g.l.]
All days	27	1404	1104	1400	192.3	722
morning	13	1995	888	1100	174.6	726
afternoon	14	1232	1251	2000	220.5	720
Events	9	1509	1300	1250	200	228
morning	5	1066	950	800	154.5	228
afternoon	4	3019	1435	1550	285.8	334
Undefined	16	1450	1129	1450	180.7	732
morning	8	2793	838	1200	182.6	728
afternoon	8	1149	1169	2000	178.7	736
Non-events	2	887	744	2000	162.3	868
morning	-	-	-	-	-	-
afternoon	2	887	744	2000	162.3	868

510

511

512

513

514

515

516

517

518
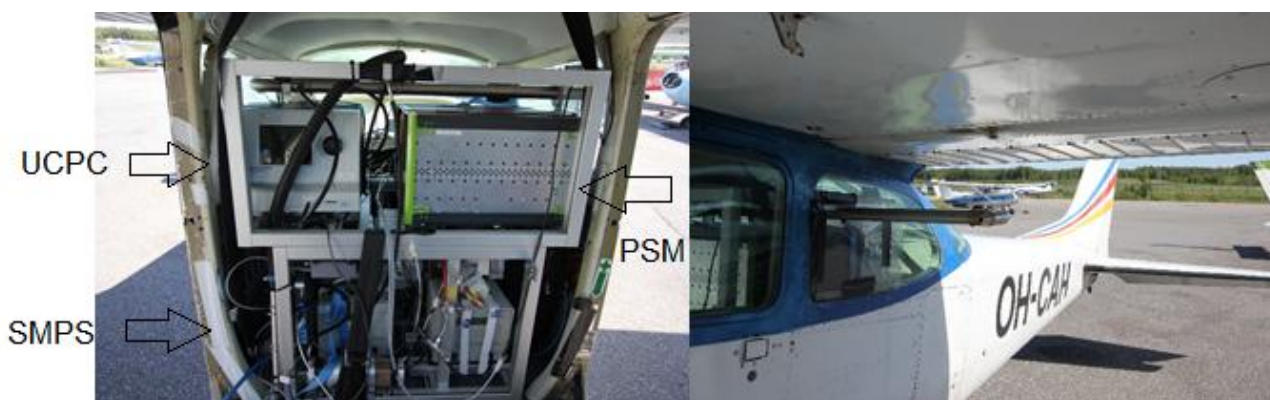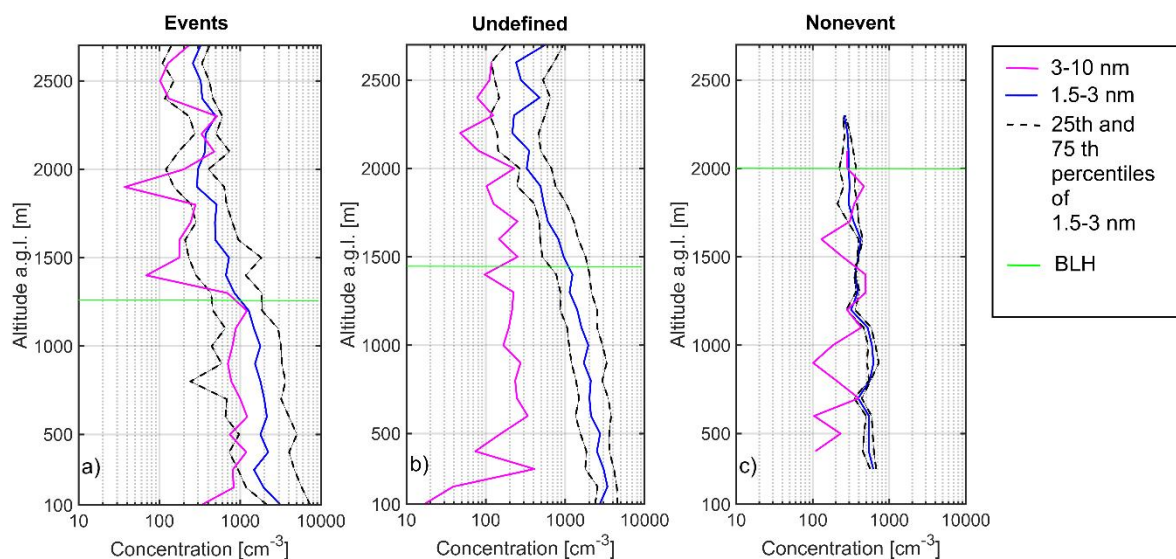
519

520

522

523

524

525

Figure 1. Instrumentation rack was installed inside the cabin (on the left) and the sample air for the instrumentation was taken from a steel tube at 50 cm distance from the fuselage of the plane (on the right). The main instruments (ultrafine-CPC, PSM and SMPS) are shown in figure.

529

530

531

Figure 2. All day median particle concentrations in two size ranges, 3–10 nm (pink) and 1.5–3 nm (blue) and 25- and 75-percentiles (dashed lines) of the 1.5–3 nm particle concentration, as a function of altitude over 17 event day (a), 34 undefined day (b) and 2 non-event day afternoon profiles (c). The concentrations were calculated from the differences between three instruments (PSM, uCPC and SMPS) at different cut-off sizes: 1.5 nm, 3 nm and 10 nm, respectively. The data were collected from near (< 30 km) to SMEAR II station during spring and August flight measurement campaigns in 2015 and spring campaign 2017. Median boundary layer heights are marked by green lines.

540
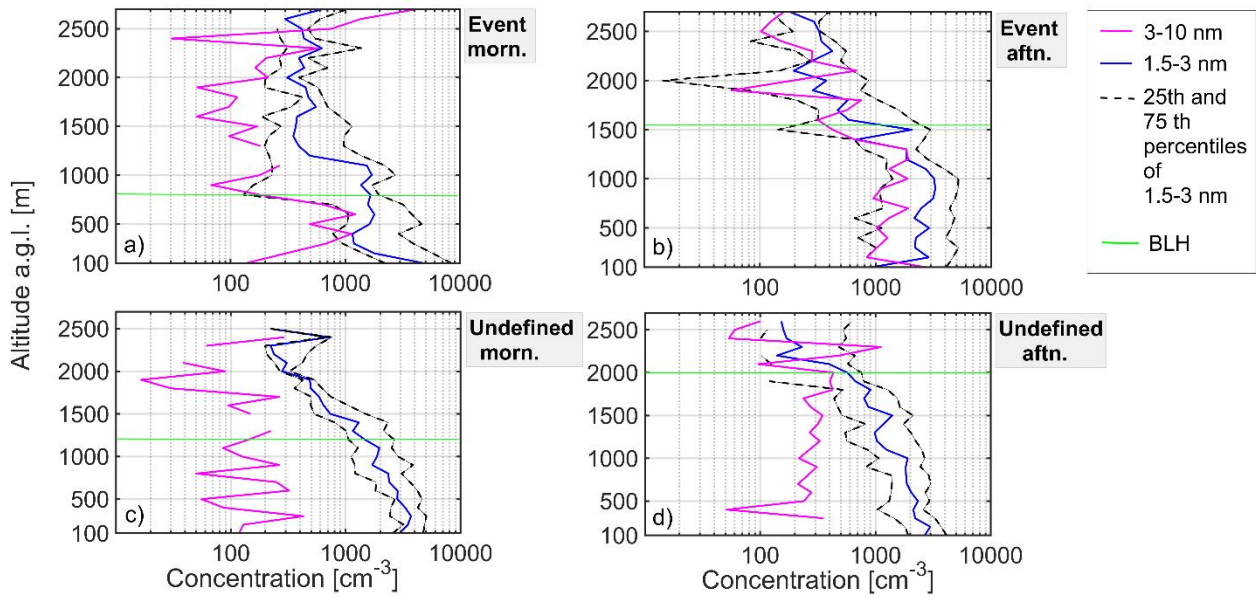
541

542

543   Figure 3. Median concentrations in two size ranges (1.5–3 nm and 3–10 nm) and 25- and 75-
544   percentiles of 1.5–3 nm particle concentration over measurement profiles during event and
545   undefined days separately for morning (a, c) (7:00–12:00 o'clock) and afternoon (b, d) (12:00–
546   15:00 o'clock) times. The median vertical profiles were defined over 9 event morning, 8 event
547   afternoon, 18 undefined morning and 16 undefined afternoon profiles. Median boundary layer
548   heights are marked by green lines.

549

550

551

552

553

554
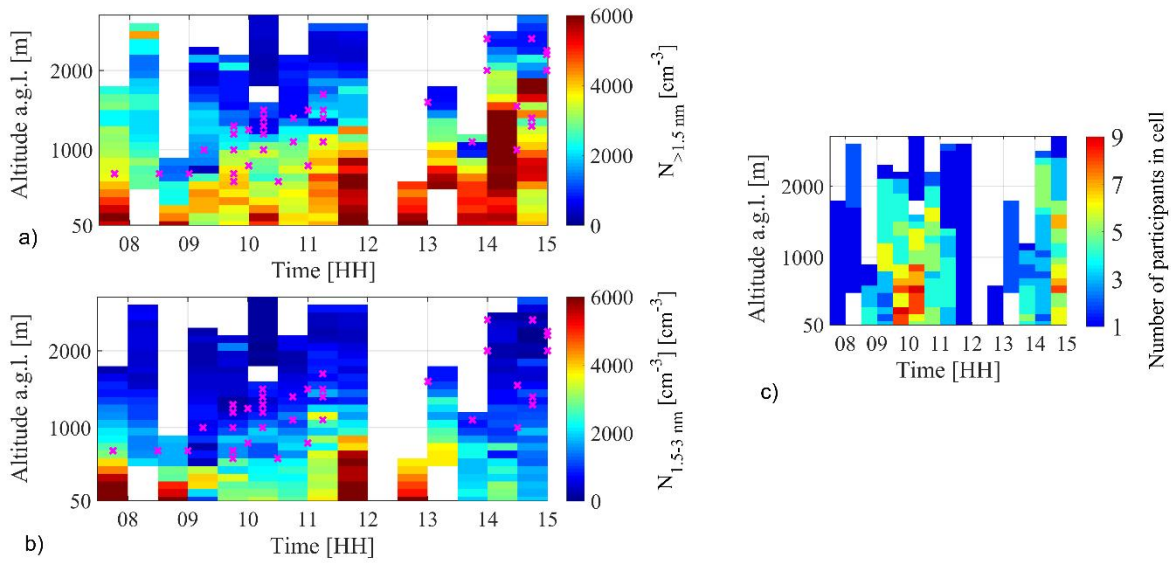
Figure 4. Panel a) shows median total particle number concentration at different altitudes calculated over 51 measurement flight profiles (17 event day and 34 undefined day profiles) during 2015 spring and August and 2017 spring campaigns in 30 km maximum distance from SMEAR II station. The total particle number concentration was measured with PSM with the cut-off size of 1.5 nm. Colour scale indicates total number concentration. Panel b) shows median particle number concentration in the size range of 1.5–3 nm at different altitudes. The value is defined as difference of total number concentrations with different cut-off sizes; PSM (1.5 nm) and uCPC (3 nm). Panel c) shows the number of data points in each cell of figures a-b). Estimated boundary layer heights are marked as crosses in figures a-b) over flight profiles. Each cell includes the median value of all measurement points inside the 100 m bin and half-an-hour.

571
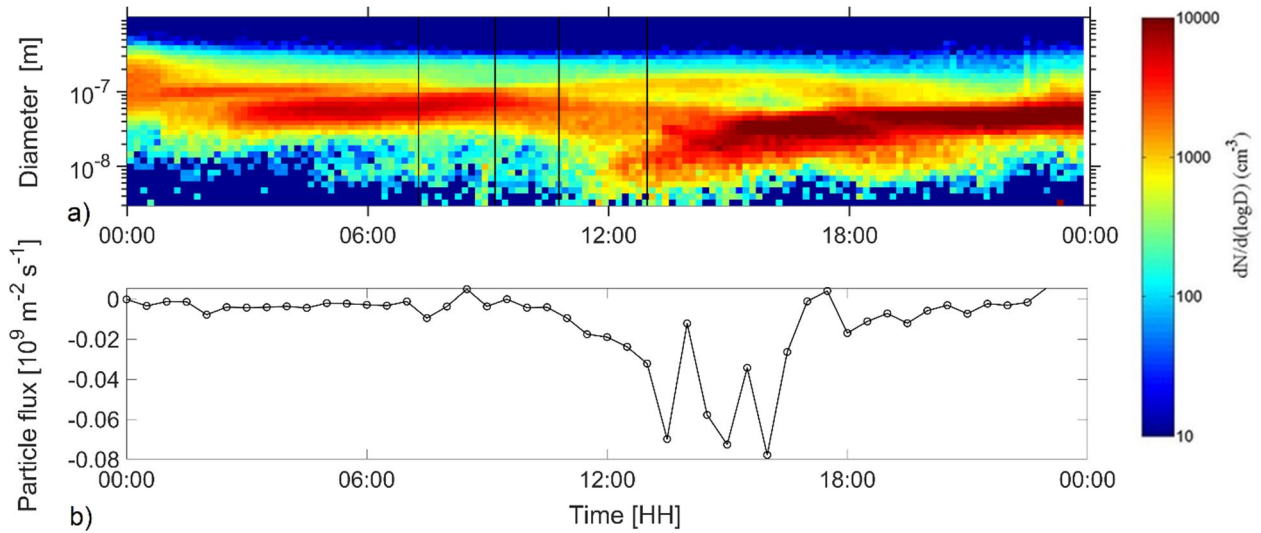
Figure 5. New particle formation event at SMEAR II station in Hyytiälä on 13ᵗʰ August 2015. Panel a) shows the number size distribution measured by Differential Mobility Particle Sizer at ground level inside the forest canopy. Start and end times of two measurement flights were marked by vertical lines in figure. Panel b shows the particle flux measured at 23 m above ground level at the station. Negative particle flux indicates particles flux downwards.

577


578
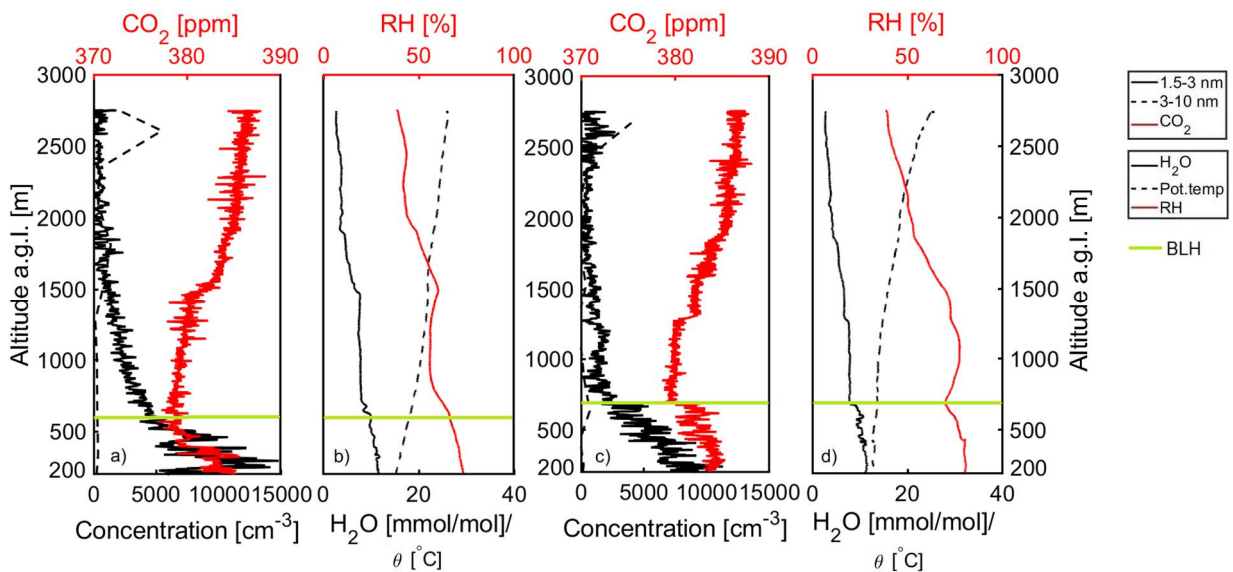
Figure 6. Vertical profiles during the first measurement flight at 7:30–9:00 a.m. on 13ᵗʰ August 2015 (marked in Fig 5). Panels a, b) show data from the ascent and c, d) from the descent. Figures a) and c) show the number concentration of 1.5–3 nm (black solid line) and 3–10 nm (dashed line) particles and the carbon dioxide concentration (red). Panels b) and d) show water vapor concentration (black), relative humidity (red) and potential temperature (dashes line) profiles. The green line is the estimated boundary layer height.

585

586
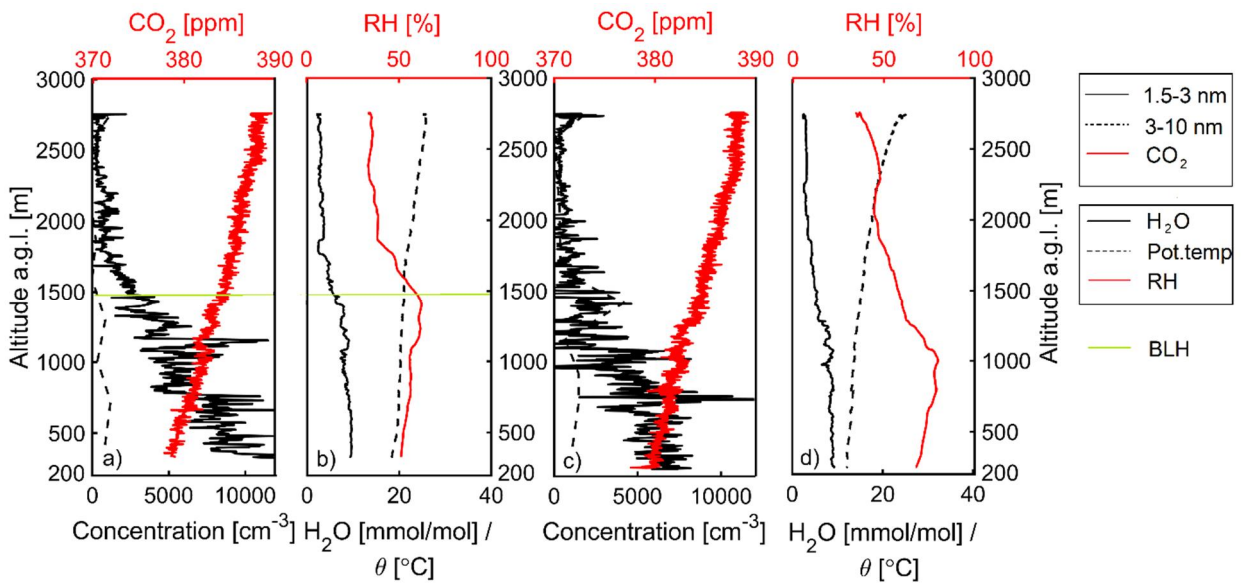
Figure 7. Measurement profiles like in the previous figure, but during the second measurement flight on 13th August 2015 at 11:00 a.m. – 12:45 p.m.